LBL-32279
UC-405

Lawrence Berkeley Laboratory

UNIVERSITY OF CALIFORNIA

Physics Division

Mathematics Department

To be presented at the Symposium on Fluid Mechanics Phenomena in Microgravity, ASME Winter Annual Meeting, Anaheim, CA, November 8-13, 1992, and to be published in the Proceedings

On Canonical Cylinder Sections for Accurate Determination of Contact Angle in Microgravity

P. Concus, R. Finn, and F. Zabihi

July 1992

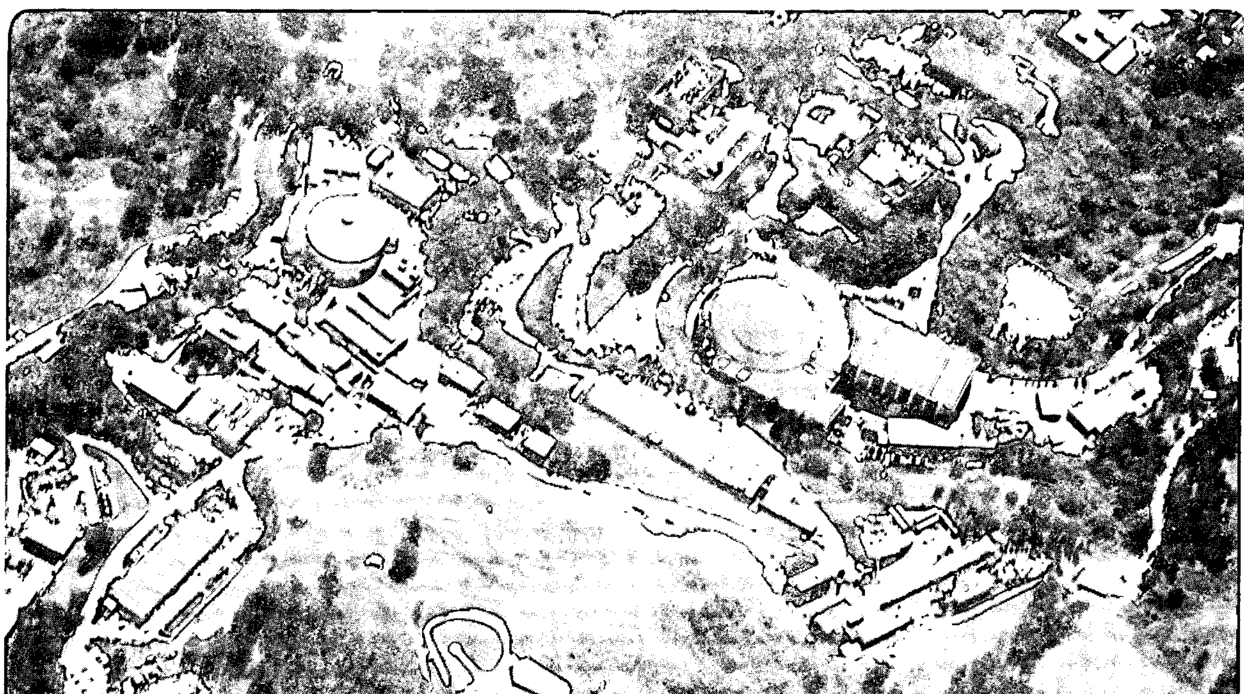

Prepared for the U.S. Department of Energy under Contract Number DE-AC03-76SF00098

LBL-32279

ON CANONICAL CYLINDER SECTIONS FOR ACCURATE DETERMINATION OF CONTACT ANGLE IN MICROGRAVITY *

Paul Concus
Lawrence Berkeley Laboratory
and
Department of Mathematics
University of California
Berkeley, California 94720

Robert Finn
Department of Mathematics
Stanford University
Stanford, California 94305

Farhad Zabihi
Lawrence Berkeley Laboratory
and
Department of Mathematics
University of California
Berkeley, California 94720

July 1992

* This work was supported in part by the Applied Mathematical Sciences Subprogram of the Office of Energy Research, Department of Energy, under Contract Number DE-AC03-76SF00098, by the National Aeronautics and Space Administration under Grant NAG3-1143, and by the National Science Foundation under Grant DMS89-02831.

ON CANONICAL CYLINDER SECTIONS FOR ACCURATE DETERMINATION OF CONTACT ANGLE IN MICROGRAVITY

Paul Concus
Lawrence Berkeley Laboratory and Department of Mathematics
University of California, Berkeley, CA 94720

Robert Finn
Department of Mathematics
Stanford University, Stanford, CA 94305

Farhad Zabihi
Lawrence Berkeley Laboratory and Department of Mathematics
University of California, Berkeley, CA 94720

ABSTRACT

Large shifts of liquid arising from small changes in certain container shapes in zero gravity can be used as a basis for accurately determining contact angle. "Canonical" geometries for this purpose, recently developed mathematically, are investigated here computationally. It is found that the desired "nearly-discontinuous" behavior can be obtained and that the shifts of liquid have sufficient volume to be readily observed.

INTRODUCTION

The behavior of an equilibrium free-surface of liquid partly filling a container can change dramatically when an external gravity field is allowed to decrease to zero. For a cylindrical container of general cross-section in zero gravity the surface change can be discontinuous or "nearly discontinuous", leading to large shifts of the liquid mass arising from small changes in geometry or contact angle. We are exploiting this behavior presently as a means for designing containers for accurate determination of contact angle. Space experiments are being planned in this connection.

The principal mathematical result providing the basis for design of the container cross-sections is that for particular cylindrical sections a discontinuous kind of change can be realized as the contact angle γ crosses a critical value γ_0. When γ is larger than γ_0 there exists an equilibrium configuration of liquid that covers the base of the cylindrical container simply, while for contact angles smaller than γ_0 no such equilibrium configuration can exist. In the latter case fluid moves to the walls and uncovers a portion of the base if the container is tall enough. A practical challenge is to design a cross-section so that a large enough portion of the fluid will rise up the walls for easy observation as the critical value of contact angle is crossed, without the container being unrealistically tall. Our studies have shown generally that (for a wetting liquid) this is more difficult to do for smaller contact angles than for larger ones.

By using two or more containers corresponding to appropriately chosen values of γ_0, differing, say, by the accuracy desired for the contact angle measurement, one can surround the value of the contact angle to be determined, and thereby, by observing on which sides of the transition the bulk fluid configurations lie, obtain the desired value. In some cases, geometries can be "combined" into a single container for determining contact angle.

Recently, Fischer and Finn have developed a family of "canonical" cross-sectional shapes for determining contact angle, for which the critical movement of fluid to the walls can be made clearly accessible to observation, even for small contact angles. Here we give results of numerical calculations of the equilibrium free surface in such containers to illustrate the behavior that might be expected over a range of contact angles of practical interest near the critical one.

GOVERNING EQUATIONS

Consider a cylindrical container of general cross-section partly filled with liquid, as indicated in Fig. 1. According to the classical Young-Laplace theory, an equilibrium interface in the absence of gravity between the liquid and gas (or between two immiscible liquids) is determined by the equations

$$\operatorname{div} Tu = \frac{1}{R_\gamma} \quad \text{in } \Omega, \tag{1}$$

$$\nu \cdot Tu = \cos\gamma \quad \text{on } \Sigma, \tag{2}$$

where

$$Tu \equiv \frac{\nabla u}{\sqrt{1+|\nabla u|^2}};$$

see, e. g., Chapter 1 of (Finn, 1986). In these equations Ω is the cross section of the cylindrical container, Σ is the boundary of Ω, ν is the exterior unit normal on Σ, and

$$R_\gamma = \frac{|\Omega|}{|\Sigma|\cos\gamma}, \tag{3}$$

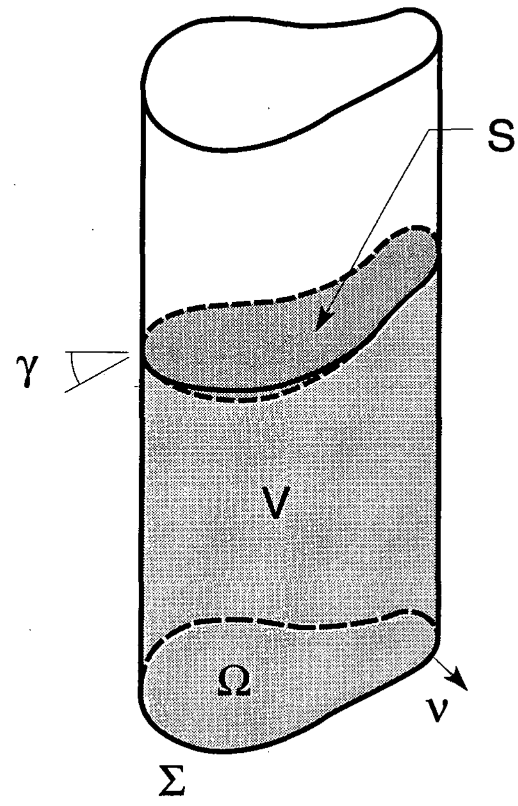

Figure 1. Partly filled cylindrical tube with base Ω.

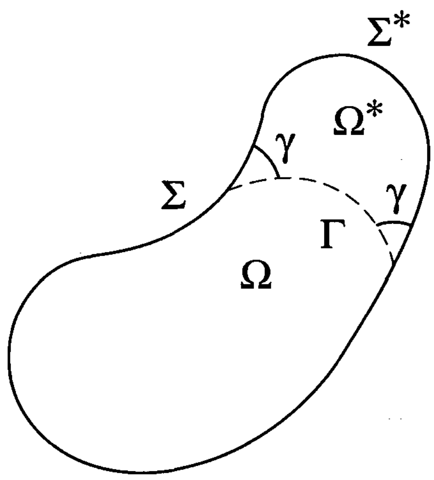

Figure 2. Domain partitioned by circular arc Γ of radius R_γ.

where $|\Omega|$ and $|\Sigma|$ denote respectively the area and length of Ω and Σ; $u(x, y)$ denotes the height (single-valued) of the interface S above a reference plane parallel to the base, and γ is the contact angle between the interface and the container wall, determined by the material properties. The volume V of liquid in contact with the base is assumed to be sufficient to cover the base entirely. We restrict discussion here to the case of a wetting liquid $0 \leq \gamma < \pi/2$ (the complementary non-wetting case can be easily transformed into this one). For $\gamma = \pi/2$, the solution surface is a horizontal plane for any cross-section.

COMPARISON THEOREM

The procedure for determination of the critical contact angle is based on the following comparison theorem; see (Finn, 1984) and (Concus and Finn, 1990b). We introduce circular arcs Γ of radius R_γ lying in Ω and joining two points of Σ; we refer to the "exterior" of Γ as the portion Ω^* of Ω cut off by Γ, that also lies exterior to the circle determined by Γ. We denote by Σ^* the part of the boundary Σ bordering Ω^*. In interpreting the following theorem reference should be made to Fig. 2. We consider Σ to consist of a finite number of smooth arcs, joining at any corner points in well defined angles. A corner point is called *reentrant* if the angle formed interior to Ω at the corner exceeds π.

THEOREM. *A solution exists for given Ω and γ if and only if, for every subarc Γ of a semicircle of radius R_γ in Ω such that each intersection point with Σ is either a reentrant corner or else a point interior to a smooth arc of Σ where Γ and Σ meet at angle γ (measured exterior to Γ) , the functional $\Phi(\Omega; \Gamma; \gamma)$ defined by*

$$\Phi \equiv |\Gamma| - |\Sigma^*| \cos\gamma + \frac{1}{R_\gamma}|\Omega^*|$$

is positive.

We refer to an arc Γ that satisfies the conditions indicated in the theorem as an "extremal", for the reason that these arcs arise in the "subsidiary" variational problem of minimizing Φ (see (Finn, 1984) and Chapter 6 of (Finn, 1986); in general such arcs are stationary, but need not minimize). The interest of the theorem derives largely from the fact that in most cases of interest only a finite number of extremals (aside from trivial rigid displacements arising from symmetries) can be found in a given domain Ω. Thus the kind of behavior to be expected can in general be predicted with only a finite number of area and length calculations, carried out for particular configurations.

The physical significance of the theorem can be described as follows. It can be shown, cf., p. 144 of (Finn, 1986), that for any Ω, there corresponds an angle γ_0, such that a solution to (1), (2) exists when $\gamma_0 < \gamma < \pi/2$, while no solution can be found when $0 \leq \gamma < \gamma_0$. The following discussion is based on a construction of particular domains Ω for which $0 < \gamma_0 < \pi/2$. It is shown in (Concus and Finn, 1987) that for $\gamma = \gamma_0$, there will be (at least) one non-null extremal Γ in Ω, with $\Phi(\Omega; \Gamma; \gamma) = 0$. For simplicity we restrict attention to those situations in which a single unique such extremal appears. For any $\gamma > \gamma_0$, every extremal Γ will yield $\Phi > 0$, and thus solution surfaces will exist. If we introduce a family of solutions $u(x, y; \gamma)$ with $\gamma \searrow \gamma_0$, then these solutions can be normalized by additive constants, so that they approach infinity throughout Ω^* and tend to a (bounded) solution surface in $\Omega \backslash \Omega^*$. We note that such solutions cannot be normalized to have constant liquid volume in a container with a bottom, and thus for any given volume V the base will become partly uncovered for some $\gamma > \gamma_0$, depending on V. Because of these striking changes, which in cases of particular interest can be nearly discontinuous, the result lends itself naturally to experimental study. Even if gravity is not strictly zero, but only close to being zero, as in an orbiting space vehicle, numerical computations indicate that the above properties obtained from zero gravity analysis will still be present.

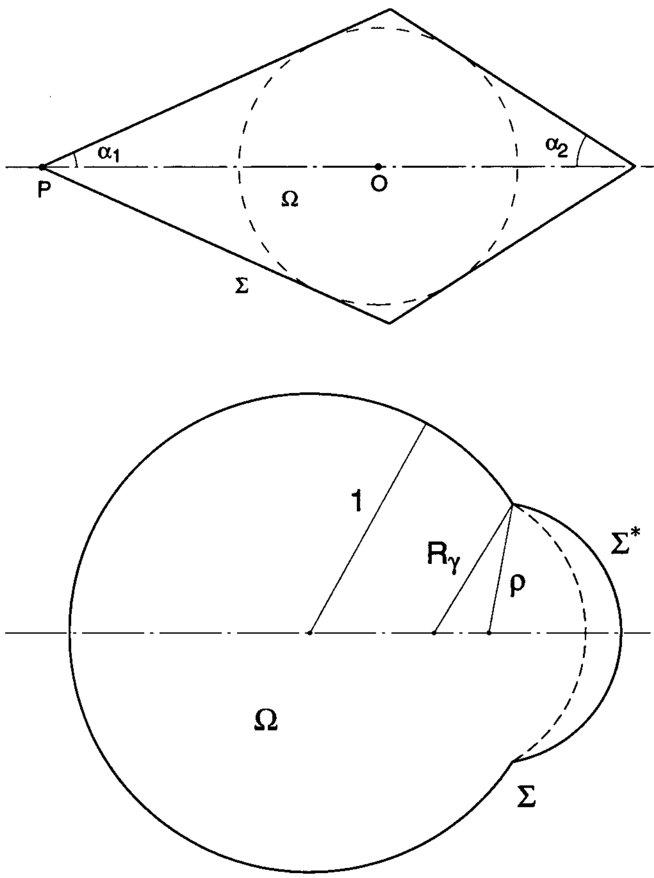

Figure 3. Near-rhombus and two-circle domains

CANONICAL SECTIONS

In previous work we have considered "near-rhombus" and "two-circle" cross-sections for the determination of contact angle in microgravity (Concus and Finn, 1991), see Fig. 3. The behavior of the near-rhombus section is based on the local condition for a wedge-shaped domain that the critical contact angle is given by $\gamma_0 = \frac{\pi}{2} - \alpha$, where α is the interior half-angle at the corner (Concus and Finn, 1974), (Concus and Finn, 1990a). The interface behaves discontinuously in this case with an abrupt transition as the value γ_0 is crossed. For the near-rhombus domain in Fig. 3, with $\alpha_1 < \alpha_2 < \pi/4$, fluid will leave the base and flow into the corner at P if $\alpha_1 < \frac{\pi}{2} - \gamma < \alpha_2$. If $\alpha_1 \geq \frac{\pi}{2} - \gamma$ then the free surface will be a lower spherical cap with center over O concentric with the inscribed circle (dashed curve) and meeting the walls in angle γ. Indications are that the near-rhombus configuration (possibly with the slight modification indicated in (Concus and Finn, 1991) for $\gamma < 45°$) can work very well for determining contact angles that exceed about 40°. For smaller contact angles the two-circle section (a larger circle with a protrusion of a portion of a smaller circle ($\rho < 1$) from it, Fig. 3) has some promise. The behavior can be nearly-discontinuous in this case, but for very small contact angles the amount of fluid participating in the flow to the wall at transition may be too small to be easily observed or to overcome such effects as container surface irregularities and hysteresis (Concus and Finn, 1991).

In (Fischer and Finn) container section geometries are developed that extend and improve on the two-circle configuration. Protrusions from the larger circle that are more general than a smaller circle are considered, which enlarge the portion of Ω over which the fluid rise at transition takes place. A canonical container section geometry is determined with a family of protrusions designed so that the sub-region Ω^* over which the fluid rises to infinity as $\gamma \searrow \gamma_0$ can be made as large as desired. This is achieved by designing the "proboscis" protrusion so that along it an entire continuum of extremals exist, as indicated in Fig. 4. The proboscis can be arbitrarily long. There holds $\Phi = 0$ for every Γ in the family of extremal arcs, and the fluid rise to infinity is over the entire proboscis to the right of the left-most extremal arc.

The canonical proboscis shapes are given in closed form in (Fischer and Finn) as

$$x = \sqrt{R_\gamma{}^2 - y^2} + R_\gamma \sin\gamma \ln \frac{\sqrt{R_\gamma{}^2 - y^2}\cos\gamma - y\sin\gamma}{R_\gamma + y\cos\gamma + \sqrt{R_\gamma{}^2 - y^2}\,\sin\gamma} + C.$$

(In the above equation and in Fig. 4 the subscript 0 has been dropped from γ in the interest of clarity of printing.) The constant C is determined by specifying the initial point (x_0, y_0) of the proboscis, and the branch of interest is for $0 \leq y < R_\gamma \cos\gamma$. R_γ must correspond to (3) for the cross section obtained when joining the proboscis to a closing boundary curve. The choice of a circular arc, as in Fig. 4, permits R_γ to be determined in a computationally convenient way. The section may be closed in other ways, for example without the introduction of reentrant corners, if desired.

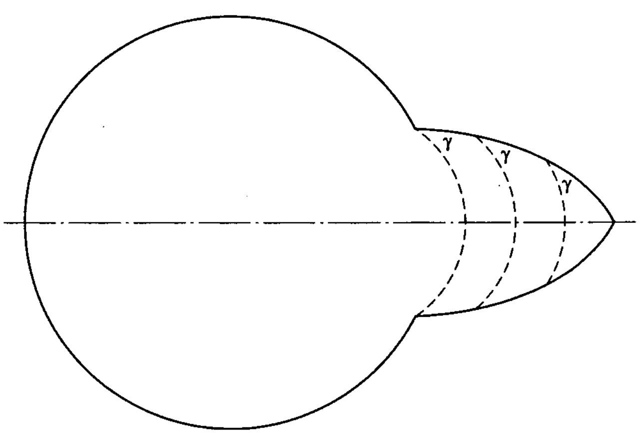

Figure 4. A canonical proboscis domain showing three members of the continuum of extremal arcs.

Of practical interest for design of a vessel for determining contact angle is the detailed behavior of the free surface as the contact angle γ decreases to the critical value γ_0. A nearly discontinuous behavior is sought for which the surface height changes slowly at first as γ_0 is approached, the increase in height then becoming substantial when γ is very near to γ_0, at which value the height becomes infinite. The amount of fluid participating in the transition at $\gamma = \gamma_0$ should be sufficient so that an easily discernible shift of liquid bulk away from the bottom and toward the proboscis wall occurs. Determination of the detailed surface is not directly amenable to mathematical analysis for domains such as in Fig. 4, but information can be obtained by numerical solution of (1), (2) for a set of values of γ decreasing toward γ_0.

NUMERICAL RESULTS

Eqs. (1), (2) were solved numerically for several canonical container shapes having different values of γ_0 and with different proboscis lengths, for a range of contact angles γ. Of principal interest were the smaller contact angles (0° to 40°), for which the near-rhombus domain would not be suitable. The adaptive-grid finite-element software package PLTMG written by Randolph Bank was used to obtain the numerical solution. A piecewise-linear approximation to the proboscis portion of the boundary was used; the circular-arc portion could be represented as such in the package.

Results are given here for three different domains corresponding to critical contact angle $\gamma_0 = 30°$. The upper half of the domain proboscides—one short, one intermediate, and one long—are shown in Fig. 5. The container cross-sections are formed by joining a proboscis to a circular arc, as depicted in Fig. 4; for the scalings in Fig. 5 the joining circular arcs have radius unity. The domains were selected to illustrate the effects of varying proboscis length for the prescribed γ_0. The results are representative generally of those obtained for the other contact angles, as well.

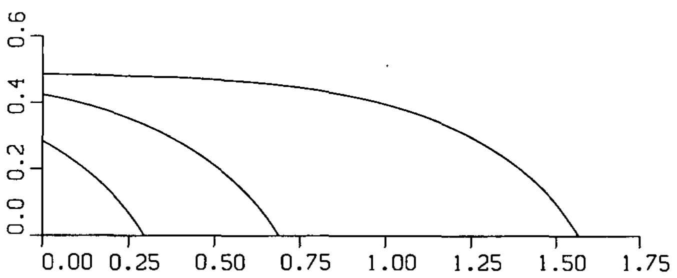

Figure 5. Upper half of the three proboscides—short, intermediate, and long—used for the numerical examples. The container cross-sections are formed by joining a proboscis to a circular arc of unit radius, as depicted in Fig. 4.

To speed the computation, only the upper half of the domain was input to PLTMG, with a reflective symmetry boundary condition $\nu \cdot \nabla u = 0$ in place of (2) along the symmetry line. Solutions were normalized by taking $u = 0$ at the center of the unit circle portion of the domain boundary.

The numerically calculated solution surface $u(x, y)$ for the (upper half of the) intermediate proboscis domain is shown in Fig. 6 for four values of contact angle, 60°, 40°, 35°, and 31°, from upper left to lower right. The three-dimensional views of the surface are color-shaded by PLTMG to indicate contour levels, grayscale versions of which are shown in the figure. The viewpoint for each surface is the same, but there may be slight variations of two or three percent in scale between them arising from the size reductions for the figure. Generally, as γ decreases toward $\gamma_0 = 30°$ more fluid moves toward and up the proboscis wall, with the maximum height, as calculated by the program, at the proboscis tip. The surfaces for the long and short proboscis domains behave similarly, with relatively larger rise height and greater amount of fluid in the long proboscis and less in the short one.

The apparent jump discontinuity in the solution height at the reentrant corner occurs in the computed solutions for contact angles smaller than a certain value, depending on the domain. (For the domain in Fig. 6 compare the surface for 60° with the others.) Such discontinuous behavior of solutions of (1), (2) at reentrant corners has been found mathematically for certain domains in (Lancaster and Siegel). The effect on the behavior of the computer program at these smaller contact angles was evidenced in the adaptive mesh refinement. Higher levels of refinement concentrated nodes in the neighborhood of the reentrant corner. Thus with the approximately 2000 nodes to which we limited the computation, relatively fewer nodes were distributed elsewhere in the domain than was the case when the discontinuity was not present. The estimate of the L^2 norm of the error given by PLTMG was, nonetheless, the order of 10^{-2} or less in all cases.

The rise height at the tip of the proboscis is shown as a function of γ for the three domains by the solid curves in Fig. 7. The calculated data, which are denoted by squares, are connected by interpolating linear segments; three of the calculated points for the intermediate proboscis domain are the ones corresponding to the surfaces in Fig. 6. At the critical value $\gamma = \gamma_0 = 30°$, denoted by the arrows, the heights would become infinite. The dashed curves show the rise height at the boundary for the circular domain with no protrusion, for which the solution is the lower spherical cap

$$u(x, y) = \left(1 - \sqrt{1 - (x^2 + y^2)\cos^2\gamma}\right)\sec\gamma,$$

which has its minimum at the origin and maximum ($\sec\gamma - \tan\gamma$) at the boundary.

For construction of a physical container for measuring contact angle, the choice of proboscis length would be governed generally by the conflicting practical requirements of not unreasonably tall container, say less than about six circle radii high, and a sufficiently large fluid shift near critical for easy observation. The latter calls for a proboscis that is not too short; the former calls for one that is not too long, so that fluid does not rise to the top of the container for contact angles too much larger, say one degree or more, than the critical one. An intermediate length would seem to give the best balance between ease of observation and ability for accurate estimate of the transition. We plan to test these designs in collaboration with D. Langbein and M. Weislogel in forthcoming space flights.

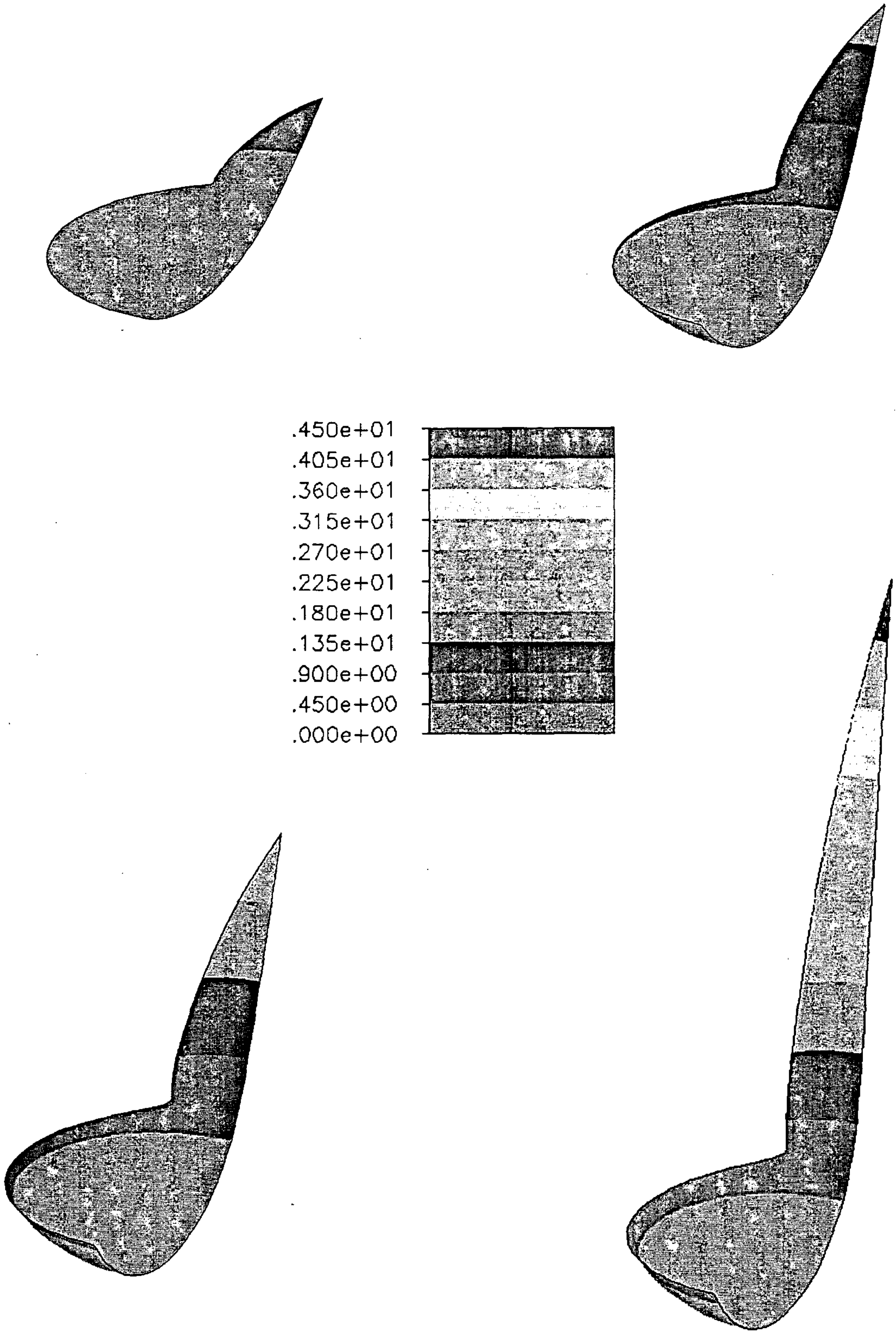

Figure 6. Equilibrium interface for the intermediate proboscis domain for contact angles 60°, 40°, 35°, and 31°. $\gamma_0 = 30°$.

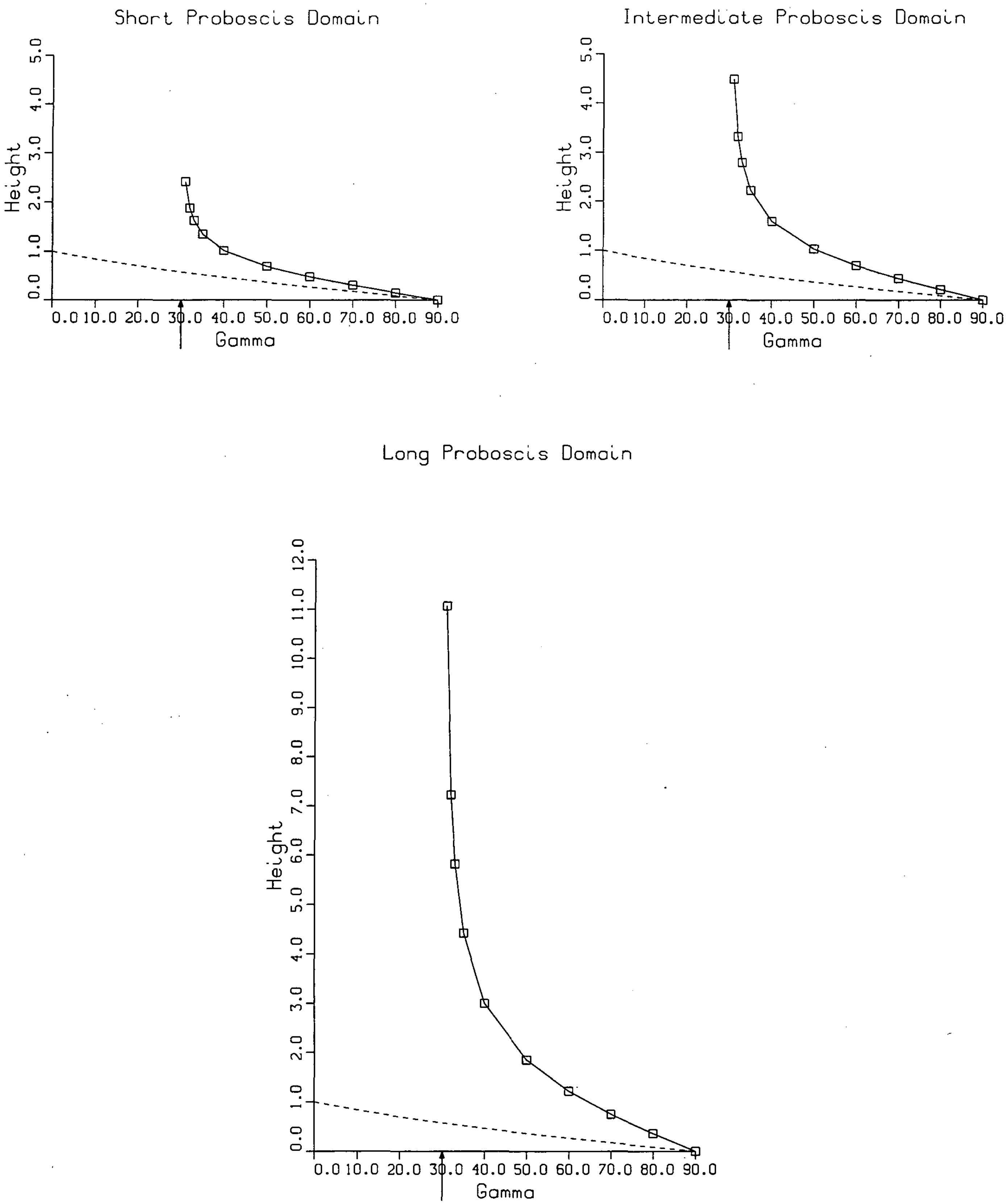

Figure 7. Maximum rise height vs. contact angle for the short, intermediate, and long proboscis domains. $\gamma_0 = 30°$.

ACKNOWLEDGMENTS

We wish to thank Randolph Bank for the personal guidance he has given us in use of the PLTMG software package. This work was supported in part by the Applied Mathematical Sciences Subprogram of the Office of Energy Research, Department of Energy, under Contract Number DE-AC03-76SF00098, by the National Aeronautics and Space Administration under Grant NAG3-1143, and by the National Science Foundation under Grant DMS89-02831.

REFERENCES

Concus, P., and Finn, R., 1974, "On capillary free surfaces in the absence of gravity," *Acta Math.*, Vol. 132, pp. 177–198.

Concus, P., and Finn, R., 1987, "Continuous and discontinuous disappearance of capillary surfaces," in *Variational Methods for Free Surface Interfaces*, P. Concus and R. Finn, eds., Springer-Verlag, New York, pp. 197–204.

Concus, P., and Finn, R., 1990a, "Capillary surfaces in microgravity," in *Low-Gravity Fluid Dynamics and Transport Phenomena*, J. N. Koster and R. L. Sani, eds., Vol. 130, Progress in Astronautics and Aeronautics, AIAA, Washington, D. C., pp. 183–205.

Concus, P., and Finn, R., 1990b, "Dichotomous behavior of capillary surfaces in zero gravity," *Microgravity Sci. Technol.*, Vol. III, pp. 87–92; Errata, Vol. III, (1991), p. 230.

Concus, P., and Finn, R., 1991, "On accurate determination of contact angle," *Microgravity Sci. Technol.*, Vol. IV, pp. 69–70 (extended abstract); Paper to appear in *Proc. IUTAM Symposium on Microgravity Fluid Mechanics, Bremen, Germany, Sept. 2-6, 1991.*

Finn, R., 1983, "Existence criteria for capillary free surfaces without gravity," *Indiana Univ. Math. J.*, Vol. 32, pp. 439–460.

Finn, R., 1984, "A subsidiary variational problem and existence criteria for capillary surfaces," *J. Reine Angew. Math.*, Vol. 353, pp. 196–214.

Finn, R., 1986, *Equilibrium Capillary Surfaces*, Springer-Verlag, New York.

Fischer, B. S., and Finn, R., "Existence theorems and measurement of the capillary contact angle," (to appear).

Lancaster, K., and Siegel, D., "Radial limits of capillary surfaces," (to appear).

LAWRENCE BERKELEY LABORATORY
UNIVERSITY OF CALIFORNIA
TECHNICAL INFORMATION DEPARTMENT
BERKELEY, CALIFORNIA 94720